^{226}Ra-^{210}Pb and ^{228}Ra-^{228}Th Dating of Barite in Submarine Hydrothermal Sulfide Deposits Collected at the Okinawa Trough and the Southern Mariana Trough

47

Ai Uchida, Shin Toyoda, Jun-ichiro Ishibashi, and Shun'ichi Nakai

Abstract

The ^{226}Ra-^{210}Pb and ^{228}Ra-^{228}Th ages were obtained for barite crystals in hydrothermal sulfide deposits taken at the Okinawa Trough and the Southern Mariana Trough. After calibrating the measurement systems with standard samples with pitchblende, it was confirmed that the U and Th concentrations obtained for GSJ samples are consistent with literature values. It was shown that radon does not escape from barite crystals extracted from hydrothermal sulfide deposits, which indicates that ^{226}Ra-^{210}Pb dating method works for these barite crystals. Most of the ^{226}Ra-^{210}Pb and ^{228}Ra-^{228}Th ages are younger than ESR and U-Th ages, where this inconsistency would be explained by the mixture of the barite crystals with younger and older ages, formed by several hydrothermal events.

Keywords

^{226}Ra-^{210}Pb and ^{228}Ra-^{228}Th ages • Barite crystals • Okinawa Trough • Southern Mariana Trough

47.1 Introduction

Determining the mineralization ages of the hydrothermal deposit will greatly contribute to the studies of temporal variation of submarine hydrothermal activities, as the ages are the essential factors to discuss ore formation process and the surrounded ecosystem sustained by the chemical species supplied by hydrothermal activities. Several dating procedures using disequilibrium of radioisotopes are available for this purpose, such as ^{238}U-^{230}Th method for sulfide minerals (Lalou et al. 1993), ^{226}Ra-^{210}Pb, and ^{228}Ra-^{228}Th methods for barite ($BaSO_4$). Noguchi et al. (2004, 2011) successfully obtained ^{226}Ra-^{210}Pb and ^{228}Ra-^{228}Th ages for barite crystals extracted from mixture of sulfide and sulfate minerals collected from the Okinawa Trough and the Southern Mariana Trough. Noguchi et al. (2011) reported the precipitation ages of hydrothermal chimneys from Izena Hole (Hakurei site) and Yaeyama Graben, by ^{226}Ra-^{210}Pb method, which range from 25 to 74 and from 14 to 53 years, respectively. Even in one chimney structure, precipitation ages are varied, which may mean the growth history of chimney structure. The ^{226}Ra-^{210}Pb ages of samples from the Southern Mariana Trough range from 30 to 35 years.

White and Rood (2001) reported that 3–20 % of ^{222}Rn is lost from the barite crystals, which are used for casing in mining. If this is the case for our barite crystals, the obtained ages will be in error. In this chapter, it is investigated if the barite crystals extracted from the sea-floor hydrothermal sulfide deposits consist of a closed system in the aspect of possible Rn loss, after confirming that the U and Th concentrations obtained for GSJ samples are consistent with literature values.

Secondly, we conducted ^{226}Ra-^{210}Pb and ^{228}Ra-^{228}Th measurements of several hydrothermal deposits collected from the Okinawa Trough and the Southern Mariana Trough.

A. Uchida • S. Toyoda (✉)
Okayama University of Science, Okayama, Japan
e-mail: toyoda@dap.ous.ac.jp

J.-i. Ishibashi
Kyushu University, Fukuoka, Japan

S. Nakai
Earthquake Research Institute, University of Tokyo, Tokyo, Japan

J.-i. Ishibashi et al. (eds.), *Subseafloor Biosphere Linked to Hydrothermal Systems: TAIGA Concept*,
DOI 10.1007/978-4-431-54865-2_47,

47.2 Experimental Procedures

47.2.1 Instruments

We used three low background gamma-ray spectrometers, which are GC1520 (CANBERRA) and EGP-100-10R (INTERTECHNIQUE) in Okayama University of Science and System 8000 (Princeton Gamma-Tech Instruments Inc.) in Kochi University. These three instruments were covered with more than 100 mm thickness of lead block to prevent the environmental gamma-ray, together with 10 mm thickness of copper plate and 5 mm thickness of acrylic plate to decrease the characteristic X-rays and/or bremsstrahlung radiations.

47.2.2 Information of Nuclides

The activities of the following radioactive nuclides were measured in the present study: ^{214}Pb (295 and 352 keV) and ^{214}Bi (610, 1,120, and 1,765 keV) which are daughter nuclides of ^{238}U, hence of ^{226}Ra, and ^{212}Pb (239 and 300 keV), ^{228}Ac (338, 911, and 969 keV),^{208}Tl (583 and 2,614 keV), and ^{212}Bi (727 keV) which are daughter nuclides of ^{232}Th, hence of ^{228}Ra.

47.2.3 Samples

47.2.3.1 GSJ Reference Materials

About 20 g of mixed standard samples (pitchblende standards) for uranium concentrations were prepared by the dilution of Proterozoic age uraninite (UO_2) from Shinkolobwe Mine in Congo, which reaches radioactive equilibrium, with NaCl or quartz (SiO_2) powder in the following contents; 51.32, 83.60, 185.83 ppm in NaCl and 46.84, 109.98, 179.45 ppm in SiO_2, respectively. The concentration of uranium in the uraninite was obtained to be 59.30 % by isotope dilution analysis using an MC-ICP-MS (Micromass, IsoProbe) (Takamasa et al. 2013). JG-3, one of GSJ (Geological Survey of Japan) reference samples (Imai et al. 1995), with Th concentration of 8.28 ppm was used as a Th standard.

Four other GSJ samples (JG-1a, JR-1, JA-2, JB-3) were measured by GC1520 based on one of the pitchblende standard in order to check if the obtained U and Th concentrations are consistent with the literature values. JG-3 was also used for this purpose for uranium concentration. All standard and GSJ samples in powder were compressed and sealed in a plastic container with a diameter of 52 mm and height of 10 mm. They were left for 14 days or more after sealing to attain radioactive equilibrium for radon. Each sample was measured for 7 days to obtain a gamma ray spectrum. Assuming radioactive equilibrium, the concentration of U was calculated from the peak intensities of ^{214}Pb (295 and 352 keV) and ^{214}Bi (610, 1,120, and 1,765 keV), and that of Th was from ^{212}Pb (239 and 300 keV), ^{228}Ac (338, 911, and 969 keV),^{208}Tl (583 and 2,614 keV),and ^{212}Bi (727.2 keV), after subtracting background, in comparison with those peaks of the standard sample.

47.2.3.2 Sulfide Deposit Samples from the Okinawa Trough and from the Southern Mariana Trough

Sulfide breccias, as shown in Table 47.1, were collected from Hatoma Knoll, Yoron Hole, and Izena Hole (Hakurei site) in the Okinawa Trough using Remote Operation Vehicle (ROV) Hyper-Dolphine of Japan Agency for Marine-Earth Science and Technology (JAMSTEC) during the

Table 47.1 Sampling locations

Sample No	Cruise	Latitude	Longitude	Depth (m)
Okinawa Trough				
Yoron Hole				
HPD#1333G06	NT11-20	27°29′383 N	127°32′001 E	591
HPD#1333G05	NT11-20	27°29′383 N	127°32′001 E	591
HPD#1333G03	NT11-20	27°29′328 N	127°32′123 E	580
HPD#1333G07	NT11-20	27°29′383 N	127°32′001 E	591
HPD#1333G08	NT11-20	27°29′383 N	127°32′001 E	591
HPD#1333G11	NT11-20	27°29′425 N	127°32′995 E	566
Hatoma Knoll				
HPD#1331G01	NT11-20	24°51′451 N	123°50′478 E	1,499
HPD#1331G07	NT11-20	24°51′520 N	123°50′559 E	1,490
Hakurei Site of Izena Hole				
HPD#1313G05	NT11-20	27°14′858 N	127°3′962 E	1,613
Southern Mariana Trough				
Archaean				
903R7-2	YK05-09	12°56′3625 N	143°37′9000 E	2,974

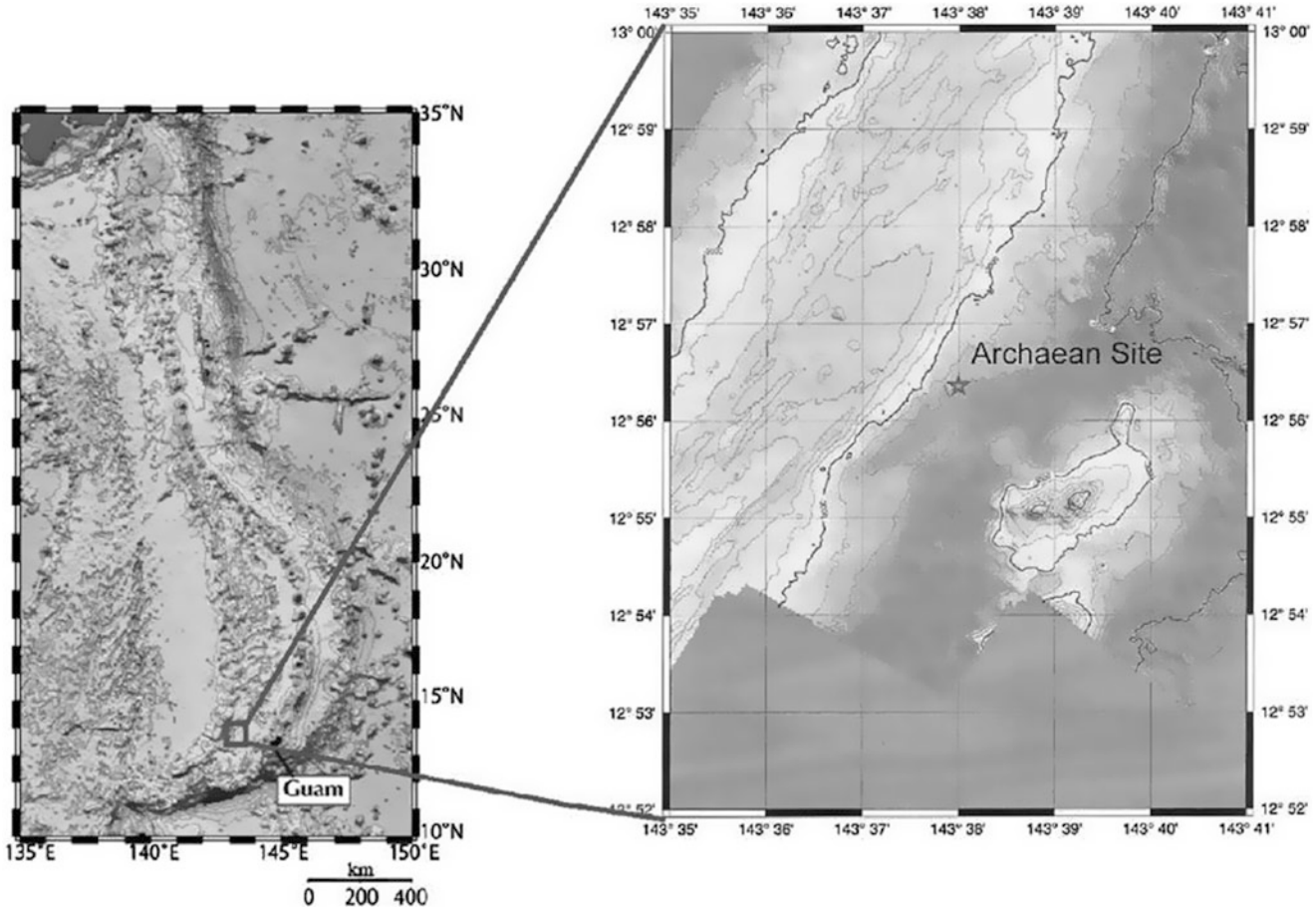

Fig. 47.1 Bathymetric chart of the Archaean site in the the Southern Mariana Trough showing the sampling site of the sulfide crust used for this study (Takamasa et al. 2013)

NT11-20 cruise in 2011 (see details in (Fujiwara et al. Chap. 29)). A sulfide chimney sample was also collected from the Archaean site in the Southern Mariana Trough by manned submersible SHINKAI6500 (JAMSTEC) during the YK05-09 cruise in 2005, the location of which is shown in Fig. 47.1.

Blocks of sulfide breccias were cut into pieces as shown in Fig. 29.3 of (Fujiwara et al. Chap. 29). Barite crystals were chemically extracted from the sulfide deposits as described in (Fujiwara et al. Chap. 29).

47.2.4 Experiments for Rn Loss

The barite crystals extracted from sample 903R7-2, dried and left for about 1 year after extraction, were packed in a columnar shape stainless container with a diameter of 100 mm, a height of 10 mm, a wall thickness of 20 mm, and a cover thickness of 1.5 mm, being sealed by two O rings between the container body and the two covers, to prevent from Rn loss. Gamma ray spectra were obtained for the crystals in the above container by EGP 800-10-R. The measurement was started immediately after sealing the container for 10 days where the spectrum was stored on each day. The ^{222}Rn activity was calculated using both ^{214}Pb (295 keV) and ^{214}Bi (610 keV) peaks. ^{214}Pb (half-life: 26.8 min) and ^{214}Bi (half-life: 19.9 min) are the daughter nuclides of ^{222}Rn (half-life: 3.82 day), therefore, these daughter nuclides are equilibrated with ^{222}Rn within 2 h.

47.2.5 ^{228}Ra-^{228}Th and ^{226}Ra-^{210}Pb Dating

For ^{228}Ra-^{228}Th dating, the bulk samples were gently crushed by agate mortar and about 20 g was sealed in a plastic container with a diameter of 52 mm and height of 10 mm. The barite crystals extracted from samples, 1333G03a and 1313G05l, were ground and about 0.3 g of them were mixed with about 20 g NaCl, then packed into a plastic container with a diameter of 52 and 10 mm in height.

The samples were measured by GC1520 for 10–24 h. JG-3 was used as the equilibrated standard. The gamma

ray peak intensities of ^{228}Ac (911 keV) and ^{212}Bi (727 keV) were obtained. As ^{228}Ac is a daughter nucleus next to ^{228}Ra with a half-life of 6.15 h much shorter than that of parent nucleus of 5.75 years, the activity of ^{228}Ac is considered to be that of ^{228}Ra. As ^{212}Bi is a daughter nucleus of ^{228}Th and the half-lives of the nuclide between these two and that of ^{212}Bi (60.6 min) are much shorter than that of ^{228}Th, 1.91 years, the activity of ^{212}Bi is considered to be that of ^{228}Th.

Activities of ^{226}Ra and ^{210}Pb were measured using IGW14023-16. The gamma-ray spectrometer was calibrated with 4.93 mg of uraninite mixed with 3.009 g of NaCl powder, whose U content is 972.6 ppm. Standard and purified barite minerals, which are diluted with powdered NaCl, are packed into a plastic tube (φ17mm and 58 mm height). The durations of measurement were 8 to 15 h for barite samples and 5 h for the standard. The peak intensities of ^{210}Pb (46.5 keV) and ^{214}Bi (610 keV) were obtained for barite samples and for the standard. Assuming radioactive equilibrium in the standard, the activity ratios of ^{210}Pb to ^{214}Bi were calculated for the barite samples. As ^{214}Bi is a nuclide after ^{226}Ra where the longest half-life of the nuclides between these two is 3.82 days of ^{222}Rn, much shorter than 1,600 years of ^{226}Ra, the activity of ^{214}Bi is considered to be that of ^{226}Ra when no Rn is lost.

47.2.6 Age Calculation

As barite crystals do not accommodate lead but radium at the time of crystallization, ^{210}Pb is accumulated, being simultaneously decaying, as time passes due to the decay of ^{226}Ra. The changes with time of the numbers of these nuclides are expressed by the differential equations,

$$\frac{dN_1}{dt} = \lambda_1 N_1 \tag{47.1}$$

$$\frac{dN_2}{dt} = -\lambda_2 N_2 + \lambda_1 N_1 \tag{47.2}$$

where
N_1: number of ^{226}Ra
N_2: number of ^{210}Pb
λ_1: decay constant ^{226}Ra, 4.33×10^{-4} year^{-1}
λ_2: decay constant of ^{210}Pb, 3.11×10^{-2} year^{-1}.

In the time scale of several 10 years, the decay of ^{226}Ra with the half-life of 1,600 years can be neglected, i.e. the number of ^{226}Ra is constant. Then, N_2 is expressed by

$$N_2 = \frac{\lambda_1}{\lambda_2} N_{10}\left(1 - e^{-\lambda_2 t}\right) \tag{47.3}$$

assuming that initial N_2 is zero.

The activity ratio, r_{Pb}, is therefore written as

$$r_{Pb} = \frac{\lambda_2 N_2}{\lambda_1 N_1} = 1 - e^{-\lambda_2 t}. \tag{47.4}$$

The age, t, is deduced to

$$t = -\frac{1}{\lambda_2} ln(1 - r_{Pb}) \tag{47.5}$$

Similarly, barite crystals do not accommodate Th but Ra at the time of crystallization. ^{228}Th is accumulated, being simultaneously decaying, as time passes due to the decay of ^{228}Ra. The changes with time of the numbers of these nuclide are expressed by the differential equations,

$$\frac{dN_1}{dt} = \lambda_1 N_1 \tag{47.6}$$

$$\frac{dN_2}{dt} = -\lambda_2 N_2 + \lambda_1 N_1 \tag{47.7}$$

where
N_1: number of ^{228}Ra
N_2: number of ^{228}Th
λ_1: decay constant ^{228}Ra, 1.21×10^{-1} year^{-1}
λ_2: decay constant of ^{228}Th, 3.62×10^{-1} year^{-1}.

The solution of these differential equations is

$$N_1 = N_{10} e^{-\lambda_1 t} \tag{47.8}$$

$$N_2 = \frac{\lambda_1}{\lambda_2 - \lambda_1} N_{10}\left(e^{-\lambda_1 t} - e^{-\lambda_2 t}\right). \tag{47.9}$$

where initial N_2 is assumed to be zero and N_{10} is the initial number of ^{228}Ra.

The activity ratio, r_{Th}, is therefore,

$$r_{Th} = \frac{\lambda_2 N_2}{\lambda_1 N_1} = \frac{\lambda_2}{\lambda_2 - \lambda_1}\left(1 - e^{(\lambda_1 - \lambda_2)t}\right) \tag{47.10}$$

The age, t, is then deduced to

$$t = \frac{1}{\lambda_1 - \lambda_2} ln\left(1 - \frac{\lambda_2 - \lambda_1}{\lambda_2} r_{Th}\right) \tag{47.11}$$

47.3 Results and Discussions

47.3.1 Matrix Effect for Pitchblende Standards

Figure 47.2 shows the obtained calibration line of ^{214}Bi (1,120 keV) using the pitchblende standards with matrices of NaCl and SiO_2. The points for both matrices are on a same line indicating no matrix effect on the count rates depending

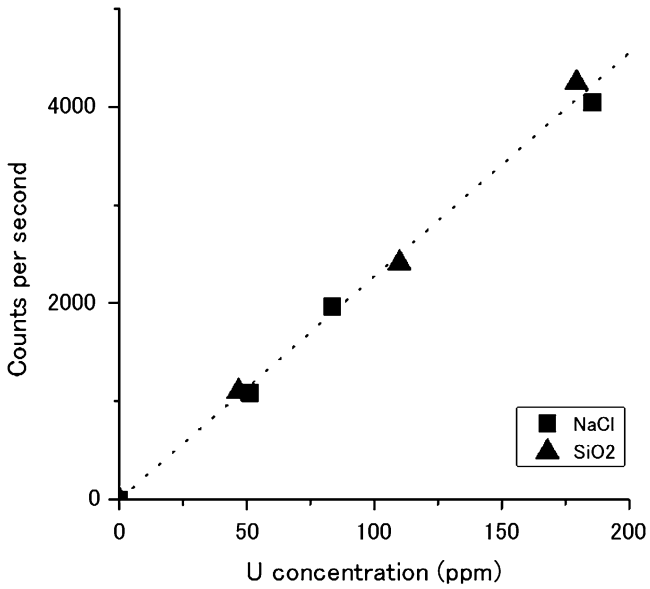

Fig. 47.2 The obtained counts for ^{214}Bi (1,120 keV) as a function of uranium concentrations in pitchblende standard samples

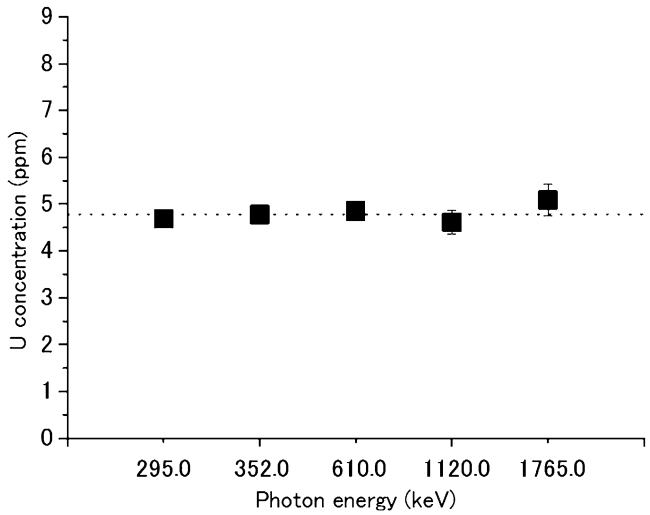

Fig. 47.3 U concentrations as a function of the gamma ray peaks. The uranium concentration was obtained as the weighted mean of these concentrations for the peaks (JG-1a)

on the matrices. One of these pitchblende standard samples, $SiO_2$110, 110 ppm of U in SiO_2, was used as the U standard for the following measurements for GSJ reference samples because the point is closest to the best-fit line.

47.3.2 GSJ Reference Materials

Each examined gamma ray peak gives the concentrations of U or Th as an example shown in Fig. 47.3. The U or Th concentration was obtained as the weighted mean of the U or Th concentrations obtained for those peaks.

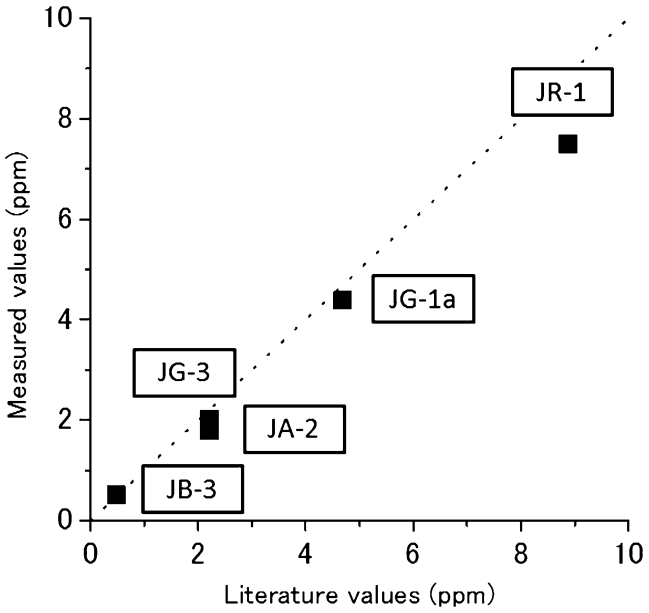

Fig. 47.4 Results of U concentration measurements for GSJ samples

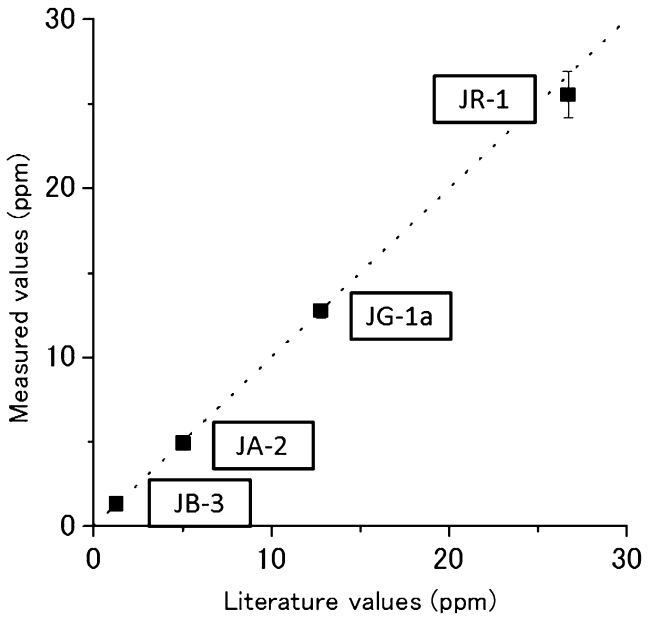

Fig. 47.5 Results of Th concentration measurements for GSJ samples

The U and Th concentrations of GSJ samples were obtained as shown in Figs. 47.4 and 47.5 plotted against the reported value (Imai et al. 1995). The broken lines indicate the one to one correlation. As for U concentrations (Fig. 47.4), the obtained values are consistent with the literature values except for JR-1. The obtained Th concentrations (Fig. 47.5) are all consistent with the literature values.

The present results show that our current system of Ge gamma ray spectrometer works well for GSJ sample assuming radioactive equilibrium except for JR-1.

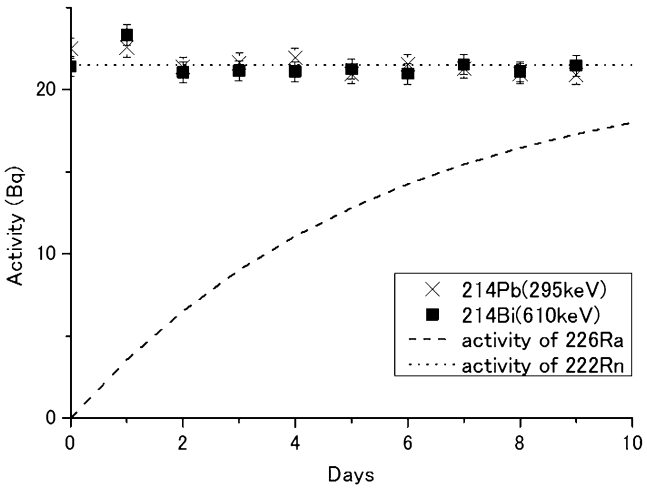

Fig. 47.6 The temporal change of the peak intensities of ^{214}Pb (295 keV) and ^{214}Bi (610 keV) observed in barite crystals after packing them in a stainless container, together with the theoretical temporal change of the activities of ^{226}Ra and ^{222}Rn. ^{226}Ra is constant in this time scale while ^{222}Rn is being accumulated as shown when 100 % is lost before packing

47.3.3 Rn Loss from Barite

Figure 47.6 shows the temporal variation of ^{214}Pb (295 keV) and ^{214}Bi (610 keV) activities of 903R7-2. If the ^{222}Rn is lost from ^{226}Ra in barite, the activities of daughter nuclides of ^{222}Rn are accumulated with time according to the following equation;

$$\frac{dN_2}{dt} = -\lambda_2 N_2 + \lambda_1 N_1 \qquad (47.12)$$

where
N_1: number of ^{226}Ra
N_2: number of ^{222}Rn
λ_1: decay constant ^{226}Ra, 4.33×10^{-4} year^{-1}
λ_2: decay constant of ^{222}Rn, 66.2 year^{-1}

The Eq. (47.12) is deduced to

$$\lambda_2 N_2 = \lambda_1 N_1 \left(1 - e^{-\lambda_2 t}\right) \qquad (47.13)$$

when initial number of N_2, ^{222}Rn, is zero, and N_1 is constant, which is an appropriate assumption as the time scale being considered is in days while the half-life of ^{222}Ra is 1,600 years.

The hypothetical ^{222}Rn accumulation with Eq. (47.13) is shown in Fig. 47.6 by the broken curves. The activities of daughter nuclides of ^{222}Rn were stable during 10 days, therefore, we conclude that there is little ^{222}Rn loss during the chemical treatment.

47.3.4 ^{226}Ra-^{210}Pb and ^{228}Ra-^{228}Th ages

^{226}Ra-^{210}Pb and ^{228}Ra-^{228}Th ages were obtained for the present samples as shown in Table 47.2.

47.3.4.1 Yoron Hole

The ^{226}Ra-^{210}Pb ages of HPD#1333G06 range $22.6^{+1.5}_{-1.4}$ to $26.7^{+1.8}_{-1.7}$ years, being more uniform than ESR ages of 70^{+10}_{-9} to 150^{+30}_{-23} years, but ^{228}Ra-^{228}Th ages are younger than those. The same order of ages with different dating methods were observed also in HPD#1333G07, HPD#1333G08, and HPD#1333G11, where the ^{228}Ra-^{228}Th ages are the youngest, then the ^{226}Ra-^{210}Pb ages, and the ESR ages are the oldest.

The ^{226}Ra-^{210}Pb ages of HPD#1333G05 are consistent within the error, from $71.4^{+11}_{-8.2}$ to 77.0^{+15}_{-10} years. The ESR ages for these samples are 200^{+30}_{-24} to 400^{+66}_{-51} years again much older. It is reasonable that, in this old sample, neither ^{228}Ra nor ^{228}Th was detected.

The ^{228}Ra-^{228}Th ages of HPD#1333G03 $4.4^{+0.81}_{-0.67}$ to $5.2^{+0.99}_{-0.80}$ years are consistent with ESR ages of $4.1^{+0.27}_{-0.26}$ to $5.2^{+0.31}_{-0.30}$ years while ^{226}Ra-^{210}Pb ages are younger to be $2.3^{+1.1}_{-1.0}$ to $3.5^{+1.1}_{-1.1}$ years. The ^{228}Ra-^{228}Th age obtained for extracted barite of HPD#1333G03a is consistent with that of the bulk measurement, indicating that extraction of barite is not necessary for ^{228}Ra-^{228}Th dating.

47.3.4.2 Hatoma Knoll

Neither ^{226}Ra-^{210}Pb nor ^{228}Ra-^{228}Th ages were obtained for HPD#1331G01 due to radioactive equilibrium, for which ESR ages are $2{,}500^{+380}_{-340}$ to $3{,}300^{+710}_{-600}$ years. The ^{228}Ra-^{228}Th age of HPD#133G07 was obtained to be $5.3^{+1.1}_{-0.85}$ years, for which ESR ages was to be $23^{+1.6}_{-1.5}$ years.

47.3.4.3 Izena Hole

As for HPD#1313G05, again, ^{228}Ra-^{228}Th ages is the youngest, then ^{226}Ra-^{210}Pb ages, and ESR age is the oldest. The ^{228}Ra-^{228}Th and ESR ages are respectively consistent within the sample (g to m) while ^{226}Ra-^{210}Pb ages are also consistent except for m. The ^{228}Ra-^{228}Th age obtained for extracted barite of HPD#1333G03l is again consistent with that of the bulk measurement.

47.3.4.4 Archaean Site of the Southern Mariana Trough

The ^{226}Ra-^{210}Pb ages of 903R7-2-08, 09, from the Southern Mariana Trough, are 99.7^{+33}_{-16} and $75.1^{+10}_{-7.7}$ years, respectively, much younger than ESR ages and U-Th ages on sulfide minerals. It is also reasonable that, in older age piece, 903R7-2-3, ^{210}Pb is in radioactive equilibrium with ^{226}Ra.

Table 47.2 Results of ^{226}Ra-^{210}Pb, ^{228}Ra-^{228}Th, ESR and U/Th dating

	^{210}Pb (Bq/g)	^{226}Ra (Bq/g)	Activity ratio of ^{210}Pb to ^{226} Ra	^{226} Ra- Pbage (years) ^{210}	^{228} Th (Bq/g)	^{228} Ra (Bq/g)	Activity ratio of ^{228} Th to ^{228} Ra	^{228} Ra- ^{228} Th age (years)	ESR age[a] (years)	U-Th age (years)
Okinawa Trough										
Yoron Hole										
HPD#1333G06b	11.5 ± 0.47	21.3 ± 0.23	0.54 ± 0.02	$24.9^{+1.7}_{-1.6}$	5.39 ± 0.43	3.90 ± 0.16	1.38 ± 0.12	$10.5^{+}_{-3.0}$\infty	70^{+10}_{-9}	
d	11.0 ± 0.48	21.9 ± 0.24	0.50 ± 0.02	$22.6^{+1.5}_{-1.4}$	3.91 ± 0.32	2.82 ± 0.12	1.39 ± 0.13	$10.8^{+}_{-3.2}$\infty	150^{+30}_{-23}	
f	12.3 ± 0.49	21.9 ± 0.24	0.56 ± 0.02	$26.7^{+1.8}_{-1.7}$	1.49 ± 0.13	1.07 ± 0.05	1.39 ± 0.14	$11.0^{+}_{-3.4}$\infty	120^{+21}_{-17}	
HPD#1333G05a	19.5 ± 0.66	21.9 ± 0.27	0.89 ± 0.03	$71.4^{+11}_{-8.2}$			nd.		330^{+60}_{-45}	
b	15.0 ± 0.53	16.7 ± 0.22	0.90 ± 0.03	$74.2^{+13}_{-9.4}$			nd.		400^{+66}_{-51}	
d	16.1 ± 0.57	17.8 ± 0.23	0.91 ± 0.03	77.0^{+15}_{-10}			nd.		200^{+30}_{-24}	
HPD#1333G03a	2.34 ± 1.05	34.2 ± 0.45	0.07 ± 0.03	$2.3^{+1.1}_{-1.0}$	65.0 ± 5.01	65.4 ± 2.60	0.99 ± 0.09	$4.5^{+0.77}_{-0.65}$	$4.6^{+0.29}_{-0.27}$	
a [b]			nm.		63.1 ± 5.07	64.0 ± 2.94	0.98 ± 0.09	$4.4^{+0.81}_{-0.67}$	$4.1^{+0.27}_{-0.26}$	
b	3.67 ± 1.07	35.2 ± 0.46	0.10 ± 0.03	3.5 ± 1.1	56.1 ± 4.30	53.9 ± 2.12	1.04 ± 0.09	$4.9^{+0.90}_{-0.74}$	$5.2^{+0.31}_{-0.30}$	
c	3.05 ± 1.05	36.3 ± 0.46	0.08 ± 0.03	2.8 ± 1.0	57.8 ± 4.41	54.1 ± 2.13	1.06 ± 0.09	$5.2^{+0.99}_{-0.80}$	$50^{+1.6}_{-1.6}$	
HPD#1333G07a	22.1 ± 0.83	34.0 ± 0.40	0.65 ± 0.03	$33.7^{+2.4}_{-2.3}$	0.78 ± 0.08	0.57 ± 0.03	1.36 ± 0.17	$9.9^{+}_{-3.3}$\infty	$52^{+1.7}_{-1.6}$	
b	20.6 ± 0.82	33.8 ± 0.40	0.61 ± 0.03	$30.2^{+2.1}_{-2.3}$	0.82 ± 0.08	0.65 ± 0.04	1.26 ± 0.15	$7.6^{+3.9}_{-2.0}$	$56^{+1.8}_{-1.7}$	
c	19.0 ± 0.78	32.5 ± 0.39	0.58 ± 0.02	$28.2^{+2.0}_{-1.9}$	0.65 ± 0.06	0.52 ± 0.03	1.26 ± 0.15	$7.6^{+3.9}_{-2.0}$	$28^{+1.2}_{-1.2}$	
d	14.7 ± 0.83	33.7 ± 0.41	0.44 ± 0.03	$18.5^{+1.5}_{-1.4}$	10.2 ± 0.79	9.15 ± 0.37	1.11 ± 0.10	$5.6^{+1.2}_{-0.93}$	$39^{+1.4}_{-1.4}$	
HPD#1333G08a	20.1 ± 0.85	36.0 ± 0.42	0.56 ± 0.02	$26.4^{+1.8}_{-1.7}$	3.00 ± 0.26	2.58 ± 0.11	1.16 ± 0.11	$6.2^{+1.6}_{-1.2}$	$35^{+1.4}_{-1.3}$	
b	15.5 ± 0.77	32.0 ± 0.39	0.49 ± 0.02	$21.4^{+1.6}_{-1.5}$	4.37 ± 0.35	3.74 ± 0.15	1.17 ± 0.11	$6.2^{+1.6}_{-1.2}$	$27^{+1.2}_{-1.2}$	
c	13.8 ± 0.77	30.8 ± 0.38	0.45 ± 0.03	19.1 ± 1.5	12.5 ± 1.04	13.1 ± 0.52	0.96 ± 0.09	$4.2^{+0.7}_{-0.62}$	$9^{+0.51}_{-0.49}$	
HPD#1333G11a	7.34 ± 1.04	36.6 ± 0.48	0.20 ± 0.03	$7.2^{+1.2}_{-1.1}$	47.3 ± 1.64	42.0 ± 1.67	1.13 ± 0.06	$5.8^{+0.71}_{-0.61}$		
Hatoma Knoll										
HPD#1331G01b	1.37 ± 0.23	1.09 ± 0.08	1.25 ± 0.23	–			nd.		3300^{+710}_{-600}	
d	1.23 ± 0.25	1.20 ± 0.08	1.02 ± 0.22	–			nd.		2400^{+300}_{-280}	
f	1.90 ± 0.31	1.85 ± 0.10	1.02 ± 0.18	–			nd.		2500^{+380}_{-340}	
HPD#1331G07			nm.		15.7 ± 1.25	14.6 ± 0.58	1.08 ± 0.10	$5.3^{+1.1}_{-0.85}$	$23^{+1.6}_{-1.5}$	

(*continued*)

Table 47.2 (continued)

	^{210}Pb (Bq/g)	^{226}Ra (Bq/g)	Activity ratio of ^{210}Pb to ^{226} Ra	^{226} Ra- Pbage (years) ^{210}	^{228} Th (Bq/g)	^{228} Ra (Bq/g)	Activity ratio of ^{228} Th to ^{228} Ra	^{228} Ra- ^{228} Th age (years)	ESR age[a] (years)	U-Th age (years)
Hakurei Site of Izena Hole										
HPD#1313G05g	3.35 ± 0.75	18.3 ± 0.31	0.18 ± 0.04	$6.5^{+1.7}_{-1.6}$	20.5 ± 1.61	15.3 ± 0.62	1.34 ± 0.12	$9.3^{+5.7}_{-2.3}$	$14^{+1.9}_{-1.5}$	
i	2.65 ± 0.73	17.3 ± 0.30	0.15 ± 0.04	5.3 ± 1.6	24.0 ± 1.85	19.1 ± 0.77	1.26 ± 0.11	$7.6^{+2.5}_{-1.6}$	$12^{+1.8}_{-1.4}$	
j	2.67 ± 0.72	18.1 ± 0.30	0.15 ± 0.04	5.1 ± 1.5	21.6 ± 1.67	16.6 ± 0.67	1.30 ± 0.11	$8.3^{+3.4}_{-1.8}$	$16^{+2.6}_{-2.0}$	
k	3.34 ± 0.71	18.0 ± 0.29	0.19 ± 0.04	$6.6^{+1.6}_{-1.5}$	17.3 ± 0.60	12.4 ± 0.51	1.40 ± 0.07	$11.1^{+5.5}_{-2.3}$	$15^{+1.8}_{-1.4}$	
l	3.39 ± 0.73	17.7 ± 0.30	0.19 ± 0.04	$6.8^{+1.7}_{-1.6}$	17.6 ± 1.40	13.2 ± 0.54	1.34 ± 0.12	$9.2^{+5.4}_{-2.3}$	$13^{+1.5}_{-1.3}$	
l[b]			nm.		22.3 ± 2.08	16.5 ± 0.83	1.35 ± 0.14	$9.6^{+15}_{-2.8}$	$14^{+1.8}_{-1.5}$	
m	4.68 ± 0.68	19.1 ± 0.29	0.24 ± 0.04	$9^{+1.6}_{-1.5}$	17.0 ± 1.41	12.4 ± 0.50	1.37 ± 0.13	$10.1^{+17}_{-2.8}$		
Southern Mariana Trough										
Archaean										
903R7-2 3	31.8 ± 0.87	30.4 ± 0.33	1.04 ± 0.03	–			nd.		1650^{+340c}_{-280}	
8	27.5 ± 0.78	28.8 ± 0.31	0.95 ± 0.03	99.7^{+33}_{-16}			nd.		780^{+90c}_{-80}	440 ± 15[c]
9	30.8 ± 0.84	34.1 ± 0.35	0.90 ± 0.03	$75.1^{+10}_{-7.7}$			nd.		370^{+50c}_{-50}	318 ± 7[c]

[a]ESR ages were obtained by (Fujiwara et al. Chap. 29)
[b]Extracted barite crystals were powdered and mixed with NaCl
[c]U-Th and ESR ages were obtained by Takamasa et al. (2013)
–: ^{226}Ra-^{210}Pb ages were not obtained due to radioactive equilibrium
nm not measured

Noguchi et al. (2011) obtained an age of 31 years by ^{226}Ra-^{210}Pb method, which is different from our results. This sample is very large about 1 m in total length as shown in Takamasa et al. (2013). The part of the sample analyzed in the present paper is different from the part analyzed by Noguchi et al. (2011). Being a different interpretation from Takamasa et al. (2013), it may be because the formation ages are different for different parts.

47.3.4.5 Comparison of the Ages Obtained by the Three Dating Methods

If the samples were formed by one single hydrothermal event, the ages obtained from ^{226}Ra-^{210}Pb, ^{228}Ra-^{228}Th, and ESR methods should coincide. However, except for HPD#1333G03, the ESR ages are older than ^{226}Ra-^{210}Pb and ^{228}Ra-^{228}Th ages. On the other hand, it is interesting the order of the ages is consistent, i.e., samples with younger ^{226}Ra-^{210}Pb or ^{228}Ra-^{228}Th ages show younger ESR ages and samples with older ^{226}Ra-^{210}Pb or ^{228}Ra-^{228}Th ages show older ESR ages. The problem in calibration of ESR ages would be one possible explanation for this. For example, if the alpha effectiveness they adopt, which is 0.043 (Toyoda et al. 2012), is different, the absolute values of ages become proportionally different. However, the ratio of the ages are not constant for the present study.

Another explanation is that the barite crystals were formed by two or more hydrothermal events and were mixed together. While the ESR method gives the averaged ages, ^{226}Ra-^{210}Pb and ^{228}Ra-^{228}Th methods give that of the last event if the parent nuclide in the crystal formed by the previous event had decayed out, as discussed by Takamasa et al. (2013). This will explain the consistency of ages of several samples, and is consistent with non-uniformity of the age ratios, i.e., HPD#1333G03 was formed by one single event about 5 years ago, while the ^{228}Ra-^{228}Th ages are those of last events and the ESR ages are the averaged ones in the cases of HPD#1333G07 and 08. This will also explain the consistency in the order of ages. When the last event is younger, the averaged age will also become younger and when the last event is older, the averaged age will also become older. For HPD#1313G05 and HPD#1333G11, such discussion may be difficult because the "averaged" (ESR) ages are not old enough for remaining ^{228}Ra to have decayed out. The similar difficulty is for HPD#1333G05 and G06 in which parent ^{226}Ra nuclide do not decay out in several hundred years. The results for HPD#1331G01 would tell that the averaged age is 2,500–3,300 years while the age of the last event is older than 150 years, above which ^{210}Pb is equilibrated with ^{226}Ra.

47.4 Conclusion

^{226}Ra-^{210}Pb and ^{228}Ra-^{228}Th ages were obtained for barite in submarine hydrothermal sulfide deposits taken at the Okinawa and the Southern Mariana Trough. Most of the ages are younger than ESR and U-Th ages, which would be explained by the mixture of young and old crystals, in the latter of which radium nuclide have decayed out. This implies that combination of ^{226}Ra-^{210}Pb, ^{228}Ra-^{228}Th and ESR or U-Th methods will more precisely tell the history of formation of sulfide deposits, i.e., the former gives the ages of younger events while the latter gives the average ages.

Acknowledgements The work was supported by TAIGA project, Grant-in-Aid for Scientific Research on innovative Areas (20109004) funded by the Ministry of Education, Culture, Sports, Science and Technology (MEXT), partly by MEXT-Supported Program for the Strategic Research Foundation at Private Universities (2011–2015, S1101036), and by the cooperative research program of Center for Advanced Marine Core Research (CMCR), Kochi University (12B039, 13A038, 13B032)

References

Imai N, Terashima S, Itoh S, Ando A (1995) 1994 Compilation of analytical data for minor and trace elements in seventeen GSJ Geochemical reference samples, "Igneous rock series". Geostand Newslett 19:135–213

Lalou C, Reyss JL, Brichet E (1993) Actinide-series disequilibrium as a tool to establish the chronology of deep-sea hydrothermal activity. Geochim Cosmochim Acta 57:1221–1231

Noguchi T, Arasaki H, Oomori T, Takada J (2004) Age determination of submarine hydrothermal barite deposits by the ^{210}Pb/^{226}Ra method. Bunseki Kagaku 53:1009–1013 (in Japanese with English abstract)

Noguchi T, Shinjo R, Ito M, Takada J, Oomori T (2011) Barite geochemistry from hydrothermal chimneys of the Okinawa Trough: insight into chimney formation and fluid/sediment interaction. J Mineral Petrol Sci 106:26–35

Takamasa A, Nakai S, Sato F, Toyoda S, Banerjee D, Ishibashi J (2013) U-Th radioactive disequilibrium and ESR dating of a barite-containing sulfide crust from South Mariana Trough. Quater Geochronol 15:38–46

Toyoda S, Sato F, Nishido H, Kayama M, Ishibashi J (2012) The alpha effectiveness of the dating ESR signal in barite. Radiat Meas 47:900–902

White GJ, Rood AS (2001) Radon emanation from NORM-contaminated pipe scale and soil at petroleum industry sites. J Environ Radioact 54:401–413